Fabrication and Characterization of Electrospun Pristine and Fluorescent Composite Poly (acrylic acid) Ultra-Fine Fibers

Jennifer S. Atchison, Caroline L. Schauer, Ph.D.

Drexel University, Philadelphia, Pennsylvania UNITED STATES

Correspondence to:
Caroline L. Schauer email: cschauer@coe.drexel.edu

ABSTRACT

Electrospinning is a facile nanofabrication technique that produces fibrous assemblies of ultra-fine fibers, 20-1000 nm in diameter, from a charged droplet of spinning solution. Optimization of the fiber diameter of a specific material system is dependent on the solution and process variables. The electrospinning parameters for poly (acrylic acid) (PAA), a synthetic polyelectrolyte, were systematically investigated and consistent nanofiber diameters with uniform morphology were achieved. The optimization matrix included several solvent systems including ethanol, aqueous NaCl and aqueous NaOH. Optimized spinning parameters were then applied to electrospinning fluorescent fibrous assembles of quantum dot-PAA ultra-fine fiber composites. Ultra-fine composite fibers were prepared by electrospinning aqueous solutions of 6wt% PAA loaded with 0.05, 0.10, 0.15 and 0.20%v/v, carboxylic acid functionalized CdSe/ZnS nanoparticles (SNPs). The resulting composite fibers exhibited uniform fiber morphologies with increasing fiber diameters corresponding to increasing SNP loading. Fluorescence micrographs reveal luminescent fibers with evenly distributed fluorophores in the higher loaded samples. Moreover, laser excited fibers manifest SNP intermittency correlated with small clusters and single SNPs suggesting excellent dispersion in the PAA matrix.

INTRODUCTION

Producing ultra-fine polyelectrolyte fibers through electrospinning has future applications in filtration, tissue engineering and sensor development [1]. Electrospinning is a facile inexpensive nanofabrication technique that results in ultra-fine fibers with diameters in the 20-1000 nm range [2]. Fibers are formed by electrifying a pendant droplet, of spinning solution, in the presence of a grounded target. The charges in the droplet redistribute due to electrostatic repulsion deforming the droplet into a Taylor cone. The cone continues to deform until a tendril forms. As tendril extends towards the grounded target the solvent evaporates and the nascent fiber experiences bending instabilities that cause the fiber to whip in the air further reducing the diameter until it is collected on the grounded target [2-3].

Substantial work has been done to correlate solution properties to fiber diameter and morphology in neutral polymer systems. Fong *et al* systematically varied the polymer concentration, net charge density and surface tension to study the formation or suppression of bead defects in aqueous polyethylene oxide solutions [4]. They reported higher viscosity favored not only uniform fiber formation but also increased the diameters of the fibers. Increasing the charge density carried by the spinning jet leads to thinner fibers with no beads and reduction of the solution surface tension leads to defect free fibers. The solvent system also has an influence on the solvent evaporation during the electrospinning process. Controlling the solvent evaporation rate during the spinning and collection phase of the process has been linked to fused fiber mats [5].

Limited electrospinning optimization studies have been reported for poly(acrylic acid) (PAA) [6]. PAA is a synthetic anionic polyelectrolyte from its carboxylate group, which makes it a simple analogue for electrospinning natural polyelectrolytes like pectin, alginate and hyaluronic acid. Kim *et al* reported a reduction in the fiber diameter when spun in an aqueous 0.01 M NaCl solution. Conversely Li *et al* reported no effect on the fiber diameters when spun in aqueous NaCl. Additionally, Li *et al* looked at the effect of PAA concentration in aqueous and dimethylformamide solutions and reported increased fiber diameters with fewer beads in higher polymer content solutions.

Additional functionality of the PAA fibrous mats can be achieved by the incorporation of nanoparticles such as fluorescent semiconductor nanoparticles (SNPs). Such fluorophores are robust against photobleaching, their emission wavelength is tunable by size and they can be rendered water-soluble by functionalizing their surface with hydrophilic moieties [7]. SNPs have both dark excitons and bright excitons expressed as fluorescence intermittency whose frequency of "on" and "off" times can be described by power law statistics. Histograms of fluorescence intensity fluctuations have been used to describe single SNP and ensemble behaviors [8].

In this work, we identify the polyelectrolyte solution properties that affect the diameter and morphology of electrospun fibers to consistently produce pristine fibers whose mean diameters are close to 60 nm. The outcome of the optimization study was used as electrospinning parameters for PAA-SNP composite fibers.

MATERIALS AND METHODS

Materials

Powdered poly (acrylic acid) (PAA) polymer ($M_w \approx$ 250,000 g/mol was used as provided by Sigma Aldrich. Water soluble Qdot® 525 ITK™ carboxyl terminated CdSe/ZnS SNPs (λ_{em} = 525) purchased from Invitrogen were used as received. Reagent grade ethanol was purchased from Sigma Aldrich. Water used in preparing samples was twice deionized to a resistivity of 18.2 MΩ/cm.

Electrospinning

Electrospinning is accomplished by electrifying a pendant droplet of spinning dope in the presence of a grounded electrode. As the surface charges on the droplet accumulate, the droplet deforms into a Taylor cone in the direction of the field with the highest charge density at the apex. When the charge density exceeds the surface tension, a jet of charged solution is ejected from the droplet. This jet is inherently unstable and as the tendril elongates the electrostatic repulsion between the charges leads to bending moments. As the fiber gets longer, the bending instabilities become more severe causing the nascent fiber to whip through the air in a helix reducing the diameter and evaporating the solvent.[4] Dry nanofibers are collected on a grounded aluminum foil electrode. The electrospinning unit consisted of a Gamma High Voltage Research power supply (0-60 KV), Harvard Apparatus 11 plus metered pump, copper screen grounded electrode, and 10 mL BD syringes with 21 gauge needles. Fibrous mats of composite and pristine fibers were collected on aluminum foil and waxed paper.

Solution Preparation

The spinning solutions for the viscosity study were prepared from 10 mL each of deionized water (18.2 MΩ•cm) and 5.0, 5.5, 6.0, 6.5, 7.0, 7.5, and 8.0 wt % PAA. The solutions were stirred for 24 h at room temperature. From each of the stock solutions 2 mL aliquots were taken and electrospun. The remaining solutions were used for viscosity, pH and conductivity measurements.

To prepare the solutions for surface tension studies reagent grade ethanol was added to deionized water to make binary solvents of 4, 10, 15, 20, 30, and 40% v/v ethanol. To each solution, PAA was added to make a 6wt% solution and stirred for 24 h. Again 2 mL aliquots were taken and electrospun. The remaining solutions were used for viscosity, contact angle, pH and conductivity testing.

Solutions for the ionization and solution conductivity studies were prepared by adding the NaOH (or NaCl (0.005, 0.01, 0.05, 0.6, 0.08, 0.1, and 0.15 M) to the deionized water and stirred for 2 h before adding PAA to make a 6 wt% solution. The polymer –solvent was mixed for 24 h. *Table I* lists the spinning parameters and ambient conditions used for each set of experiments.

TABLE I.

Sample	KV	TD	PR	T	RH
Concentration Series	11	12	0.5	22	38
Surface Tension Study	11	12	0.5	22	40
15% v/v	7	12	0.5	22	36
20-40%v/v	5	12	0.5	22	37
Charge Density Study	11	12	0.5	22	37
Ionization study	10	10	0.8	22	23
Composite Mats	9	12	0.02	21	22

KV-Potential on the droplet in KV
TD - Distance to the grounded electrode in cm
PR – pump rate in mL/HR
T – ambient temperature in °C
RH - % relative humidity

The SNP-polymer solutions were prepared by adding 15 or 20 µL of 8µM stock solution of Qdot 525 to 10 mL of deionized water. Each suspension was sonicated for 3 min and 2 mL of the suspension was kept in reserve for spectroscopy. To the remaining 8 mL of solution, 511 mg of PAA was

added for a polymer content of 6wt%. The PAA-Qdot 525 solutions were mixed for 24 h until the polymer was completely solvated.

CHARACTERIZATION

Conductivity

Solution conductivities were measured with OakTon Con 510 bench top meter and acidity was measured with Mettler Toledo Delta 320 pH meter.

Optical

Absorption and photoluminescence (PL) spectra were taken with Ocean Optics USB 2000 UV-VIS spectrometer with a DH 2000 Deuterium Tungsten Halogen light source (absorption spectra) and UV long wavelength lamp (λ = 360 nm) for PL spectroscopy.

Rheometry

Viscosity was measured with a TA Instrument AR Rheometer with the 1° cone and plate geometry at ambient temperature.

Surface Tension

Contact angle measurements were done on a custom built system and analyzed with ImageJ software with the Contact angle plug-in.

Morphology

Fiber morphology was visualized with a Ziess VP 5 Supra scanning electron microscope (SEM). The SEM samples were prepared by sputter coating, Denton Vacuum, with Pt/Pd target at 40 milli amps for 35s resulting in a 7-8 nm conductive film. The accelerating voltage was 3.5 KV at 11mm working distance in high vacuum.

Fluorometry

Steady state and time resolved fluorometry measurements were performed on a PTI Spectro-fluorometer system. The steady state fluorometer utilized double monochromator to select the excitation and filter the emission wavelength and was modified with a Teflon sample holder.

Time resolved fluorometry used a nitrogen laser generated 1 ns pulse at 337 nm at a pulse repetition rate of 10 Hz. The resulting fluorescence decay curves were fitted to an exponential decay, shown below, and the excited lifetime of the SNPs were extracted from the fitted data.

$$D(t) = \sum_i a_i \exp(\frac{-t}{\tau_i}) \quad (1)$$

Where D(t) is the delta function generated decay at time, t, and τ, is the excited lifetime of the SNP.

Laser excitation fluorescence microscopy was accomplished using a custom scanning laser fluorescence system built around an inverted optical microscope (Olympus IX 71) with fluorescence filter carousel. (*Figure 1*) Illumination is achieved by coupling a 405nm laser to a fiber optic cable routed to the side port of the microscope where the fiber output is expanded and collimated to fill the back aperture of a 40x or 100x 1.4 N.A objective.

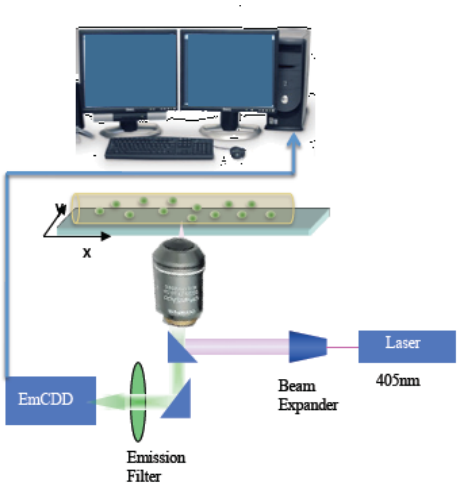

FIGURE 1. Schematic diagram of the custom built laser excitation fluorescence microscope.

The standard excitation filters and dichroic are removed from the excitation path when the laser is used. Band pass filters on the collection side select the emission wavelengths and suppress the laser excitation. Fluorescence photons are detected with an Electron Multiplying Charge Coupled Device (EmCCD) camera (Andor Luca). The EmCCD innately provides spatial context, single photon sensitivity (max quantum efficiency of 65 percent with 1-18 electron read noise depending on read out rate) and the capability to collect time series at 12.5 frames per second. The output from the EmCCD camera is connected to a computer and commercial software (Andor Solis) is used to display and analyze the images.

RESULTS AND DISCUSSION

Optimization of Poly(acrylic acid) (PAA) Fiber Diameters

Four series of solutions were prepared for the electrospinning optimization study: (1) PAA solvated in deionized water, (2) PAA solvated in a mixture of reagent grade ethanol and deionized

water, (3) PAA solvated in a mixture of NaCl and deionized water, and (4) PAA solvated and NaOH. To characterize the morphology of the resulting fibers, SEM micrographs were taken of each of the samples and the fiber diameters were measured using Image J. The populations of fiber diameters were described by plotting histograms of the distributions.

Effect of Solution Viscosity

The rheological properties of polyelectrolytes are dependent on the degree of ionization**,** in this series the PAA was solvated in water and had an average pH of 2.85 indicating less than 10 % of the carboxyl groups were ionized [9]. The increasing solution viscosity was primarily due to the increase in polymer content. In *Figure 2*, the SEM micrographs illustrate the change in the morphology of the fibers and the fiber diameter distributions of this series of increasing polymer concentrations. As the viscosity increases, the fiber diameter increases in a power law relationship to the specific viscosity (*Figure 2h)*. Additionally the morphology of the fibers goes from spherical beads to spindle beads to uniform fibers. The fibers produced from 6wt% PAA (*Figure 2b*) were close to being uniform with fiber diameters close to 60 nm. For the rest of the optimization studies 6wt% PAA was used.

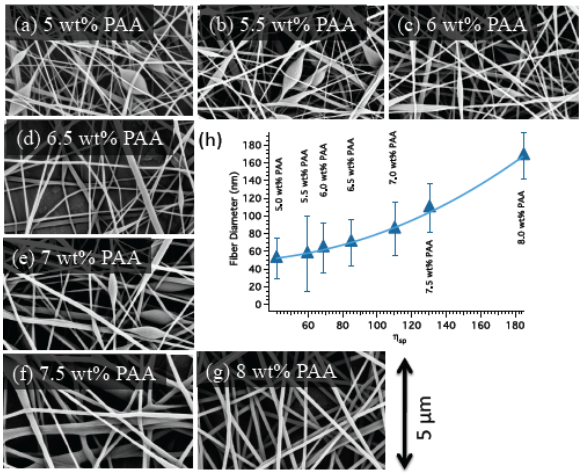

FIGURE 2. SEM micrographs of the fibers spun from (a) 5 wt%, (b) 5.5 wt%, (c) 6 wt% (d) 6.5 wt%, (e) 7 wt%, (f) 7.5 wt% and (g) 8 wt% PAA. Increasing the concentration increases the viscosity, resulting in a transition from tiny beaded fibers to elongated spindle like defects to uniform fiber diameters. Fiber diameters also increase as the fibers become more uniform. The plot in (h) illustrates the relationship between the specific viscosity and the fiber diameters.

Effect of Solution Surface Tension

To lower the surface tension of the solution, ethanol (γ_{ETOH} = 22.3 mNm^{-1}) was added to the deionized water (γ_{H2O} = 72.3 mNm^{-1}) before solvating the PAA. The solution properties and fiber mean fiber diameters are summarized in *Figure 3*. The conductivity of the solution decreased as well because ethanol is more resistive than water. The average pH was still 2.82 indicating the ethanol did not affect the ionization of the PAA chain. It is interesting to note the viscosity of the PAA solution increased with increasing ethanol content. In addition to having a lower surface tension ethanol is less polar and has lower relative dielectric constant, 24 at 25°C in contrast to water which is 80 at 20°C, the lower dielectric affects the electrostatic potential of the carboxyl group. The electrostatic potential Energy (E) is inversely proportional to the dielectric constant (ε) of the solvent and the interatomic spacing (a) between the carboxyl moiety and the counter ion.

$$E = -\frac{e^2}{\varepsilon a} \qquad (2)$$

In the case where the electrostatic potential E < kT ion dissociation is favored, in the case where E > kT ion condensation is favored. Associated ions form dipoles that aggregate into charge clusters. These clusters form between chains as well as along the chin backbone pinning the chains together [10]. This chain pinning increases with higher ethanol content, as seen by the increased viscosity, resulting in larger mean fiber diameters. The SEM micrographs revealed increasing fiber diameters with increasing ethanol content, which is not surprising in light of the increasing viscosity. The fiber morphology did evolve as the surface tension decreased from spherical beaded fibers to spindle beaded fibers to uniform fiber diameters and finally ribbon morphology with buckling jet patterning as shown in *Figure 3(i)* [11].

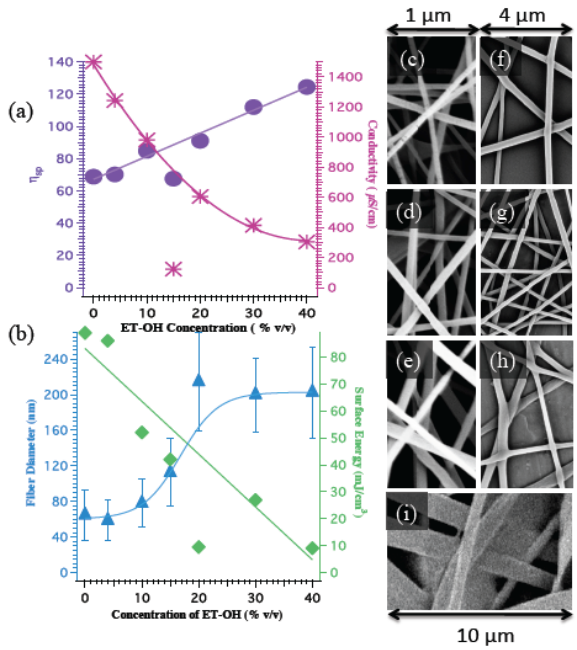

FIGURE 3. Graphs (a) and (b) plot the solution properties and fiber diameters of the fibers spun from ethanol solutions. Addition of ETOH was intended to lower the surface tension and SEM micrographs (c) through (i) illustrate the effect of increasing the concentration from (c) 4% v/v, (d) 10% v/v, (e) 15%v/v, (f) 20% v/v, (g) 30 % v/v, to (g) 40% v/v ETOH. The fiber diameters increased with increasing ETOH in the solution and above 15% v/v ETOH additional ribbon morphology was found in the mats (i) due to buckling of the jets.

Effect of Solution Conductivity

Sodium chloride was added to the PAA solution to increase the conductivity and therefore the charge carrying capacity during electrospinning. The NaCl did increase the conductivity as shown in *Figure 4* however did not have an effect on the viscosity nor did it significantly increase or decrease the fiber diameters most likely due to mild screening of the fixed charges on the slightly deprontated PAA. The standard deviations of the fiber diameter distributions overlap suggesting there is little or no effect on fiber diameters when salt is added even though there is a slight increase in the mean fiber diameter. The overall yield was significantly affected as well as the morphology of the fibers. The fibers were fused and did not have a uniform diameter, although there were no beads.

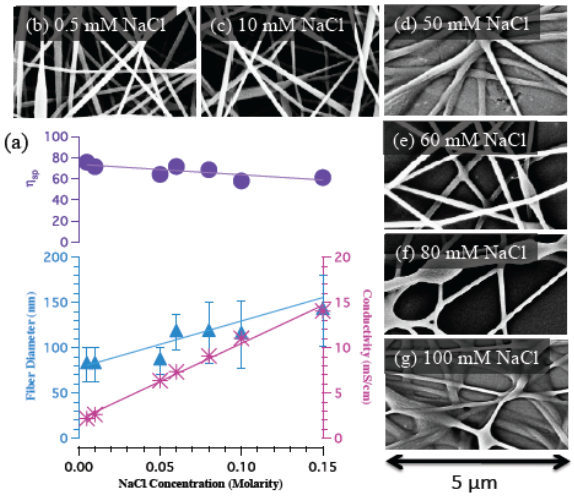

FIGURE 4. Plots (a) of the solution properties and fiber diameters examining the effect of solution conductivity. Although the fibers were not statistically different, the morphology changed with increasing salt content as seen in SEM micrographs (b) through (g).

Effect of Polyelectrolyte Ionization

One of the most important properties of polyelectrolytes is the ability to ionize the functional groups and charge the polymer chain. To ionize the anions on PAA the pH of the solution must be adjusted to exceed the pK_a of the carboxylic acid groups.

In this study, NaOH solutions were prepared at different weight percents and PAA was added. The conductivity, pH and specific viscosity were measured and plotted in *Figure 5*. As expected the conductivity increased with increasing pH and the viscosity also increased resulting in two populations of fiber diameters. At low pHs the fiber diameters are clustered around 140 nm and at high pHs the fiber diameters are clustered around 540 nm. At pH 6, the chains are more than 90% ionized and viscosity and fiber diameter increase as the chains reaches 100% ionization. The addition of higher concentrations of Na^+ ions results in counter ion condensation and screening of the charges on the polyelectrolyte chain. There is a commensurate decrease in viscosity, as well as the mean fiber diameters. The quality of the fibers also decreases as was observed the NaCl study.

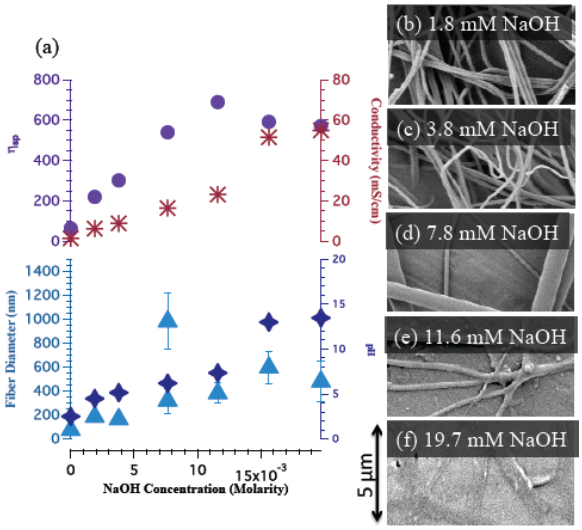

FIGURE 5. Plots (a) of the solution properties and fiber diameters. The fibers produced from the (d) 7.67mM (pH 5.76) had a bimodal distribution. The SEM micrographs of the fibers (b) through (f) illustrate the change in morphology as the polyelectrolyte became more ionized. The fiber diameters increase and the yield decreased with increasing pH.

PAA-SNP Composite Solution Preparation

The solutions containing the Qdot 525 SNPs were prepared by adding 5, 10, 15 or 20 µL of 8µM Qdot 525s solution to 10 mL of deionized water. Each suspension was sonicated for 3 minutes, and then 2 mL of the suspensions were kept in reserve for spectroscopy. To the remaining 8 mL of solution, PAA was added for a total polymer content of 6wt%. To completely solvate the polymer the PAA-Qdot 525 solutions were mixed for 24 h.

Composite Fabrication and Characterization

As previously described, the SEM micrographs reveal fibers with uniform diameters, transmission electron microscopy, reveal the quantum dots are in the fibers as single particles and small clusters [12]. The mean diameters of the fibers are 2-3 times larger than the pristine 6wt% fibers however the diameter distributions overlap suggesting there is little difference in the fiber diameters with increasing quantum dot loading as seen in *Figure 6*. However, there are less bead defects in the high Qdot 525 loadings.

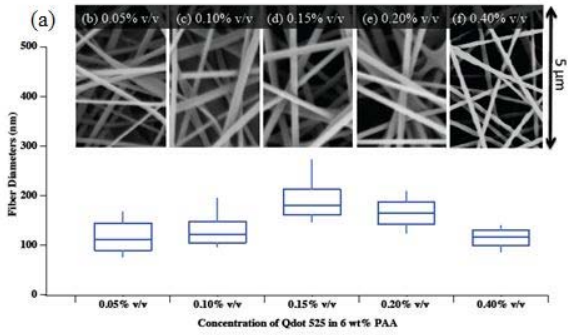

FIGURE 6. The box plots (a) of fiber diameters illustrate that increasing the loading of SNPs did not significantly affect the fiber diameters. SEM micrographs (b) through (f) reveal uniform fiber diameters for composite fibers spun from 6wt% PAA.

SNP-PAA Composite Optical Characterization

Steady state fluorescence measurements of the composite fibers exhibited band edge fluorescence at 523 nm with a FWHM of 24 nm, which is slightly red shifted and broader than the SNP-PAA solution (λ_{em}= 522 nm and FWHM = 20 nm) or the SNPs in water (λ_{em}= 521 nm and FWHM = 20 nm). The broadening is expected for SNPs confined in ultra-fine fibers [13]. Additionally the excited lifetimes of the SNPs in the fibers were measured and compared to the stock aqueous SNP solution and the aqueous PAA–SNP mixture. The lifetime of the SNP composite fibers was shorter (τ = 14.11 ns ± 0.25 ns chi ^{2} = 0.7126) than the SNP-PAA solution (τ = 19.6 ns ± 0.42 ns chi ^{2} = 1.089) and stock aqueous SNP solution (τ = 20.44 ns ± 0.1933 ns chi ^{2} = 1.113) indicating there is a change in the exciton dynamics in the fiber. The change in exciton dynamics may be due to polymer-qdot interactions or there is some work suggesting the confinement in the fibers is altering the excited lifetime by introducing a new relaxation pathway [13]. All fluorescence measurements were taken using a 366 nm excitation source.

To further explore the optical behavior of the quantum dots in the fibers and assess the dispersity of the dots, laser fluorescence microscopy was employed. In this technique, a diffraction limited laser (λ_{em}=405 nm) spot was focused on a fiber and the fluorescence was collected and filtered to remove the excitation photons while passing light centered at 530 nm. The fluorescence was detected by an EMCCD camera, which is not only exquisitely sensitive in low light applications but provided sufficient spatial discrimination to detect single and few SNPs in a fiber.

A series of images were taken at 100 ms intervals on a fiber electrospun on to a glass slide from the 10μL SNP solution and the photon trajectories were extracted for three regions of interest (ROIs). The ROIs were 5x5 pixel squares, although for illustration purposes in *Figure 7* the ROIs are identified with yellow circles. The photon counts were plotted against time as seen in *Figure 7*. Histograms of the photon trajectories intensities were plotted. The histograms revealed sub populations within the distributions. To determine the threshold for an emitter "on" state the mean (μ_{dark}) and standard deviation (σ_{dark}) for the region without emitters was taken and the "on" threshold was taken to be

$$T = \mu_{dark} + 5\sigma_{dark} \tag{3}$$

The threshold for this series was set at 63 counts. Any counts above this level are considered to be an "on" state. However, the trajectories do not display the characteristic bi-level on–off intermittency of isolated single emitters so it is assumed there is more than one emitter in each of the ROIs.

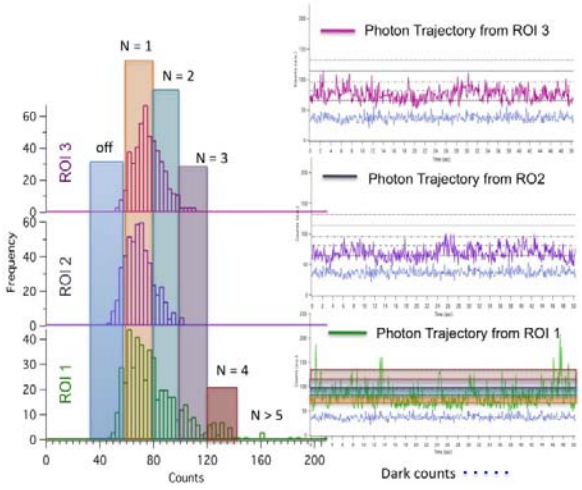

FIGURE 7. The plots on the right display the photon trajectories and on the left are the corresponding histograms. The histograms are subdivided to illustrate the subpopulations that correspond to one emitter "on" (N=1), N=2 emitters "on" up to N=5 emitters. The ROIs analyzed in this figure are displayed in *Figure 8*.

To determine the number of emitters quintile analysis was applied to the histograms. The upper bound of the first quintile corresponded to the threshold for an "on" state. The second quintile nicely bounded the first sub population in the histogram. The third, fourth and fifth quintiles similarly bounded the other subpopulations. We have assigned the second quintile to single emitters "on", third to two emitters, fourth and fifth to three and four emitters respectively. The remaining points represent more than five emitters "on" simultaneously. Previous work [12] has demonstrated that the SNPs are distributed evenly throughout the fibers in single dots or small clusters due to the carboxylic acid groups on the surface of the SNP hydrogen bonding to the partially ionized PAA.

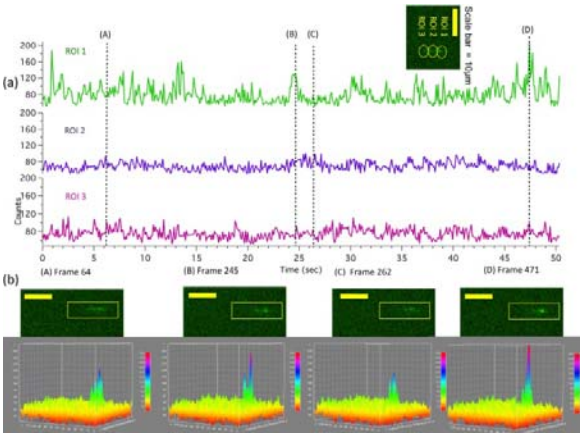

FIGURE 8. The photon trajectories (a) analyzed in *Figure 7* are plotted again to visualize in 3-D the intensity fluctuations.

Plotting the image series in 3-D (Image J) reveals ensemble blinking represented by time varying intensity changes. (*Figure 8*) The maximum intensities are associated with several SNPs turning on at the same time. Moreover, the highest frequency of counts is associated with one emitter on suggesting the SNPs are well dispersed in the fiber. This analysis was applied to ROI 1 initially and applied without modification to the other two ROIs in the image.

CONCLUSIONS

The single strongest predictor of fiber diameter in anionic polyelectrolytes is the viscosity. The solution properties that control the rheological behavior of the polyelectrolyte will control the fiber diameters. In PAA water systems, the fibers with the smallest diameters were spun from the free acid form of PAA. Fiber diameters can be controlled by changing the pH of the spinning solution or by varying the counter ion concentration. The morphology the fibers can be changed by adjusting the surface tension. Significantly lowering the surface tension leads to stabilization of the electrospinning jet resulting in ribbon morphology and jet buckling patterning.

Composite fibers of PAA and SNPs were successfully spun and optically characterized. The SNPs remained optically active in the fibers and demonstrated evidence of confinement in the PL and excited lifetimes in fibers with diameters <200 nm. SNP dispersion and optical behavior were analyzed with laser fluorescence microscopy. Results indicate the SNPs are dispersed in small clusters of less than five dots and as isolated dots.

ACKNOWLEDGEMENTS

This material is based in part on work supported by the National Science Foundation under grant numbers CMMI 0804543 and DUE 0942834. Any opinions, findings, and conclusions or recommendations expressed in this material are those of the authors and do not necessarily reflect the views of the National Science Foundation. The authors would like to thank Steve Wrenn and Eleanor Small for use of the steady state and time resolved fluorometers and fluorescence microscope, Jon Spanier for donating the Qdot 525s and use of the laser excited inverted optical fluorescence microscope. The authors would also like to acknowledge the Centralized Research Facilities at Drexel University especially Ed Basgall for training on the SEM.

REFERENCES

[1] (a) Schiffman, J. D.; Schauer, C. L., A review: Electrospinning of biopolymer nanofibers and their applications. *Polymer Reviews* 2008, *48* (2), 317-352; (b) Chunder, A.; Sarkar, S.; Yu, Y.; Zhai, L., Fabrication of ultrathin polyelectrolyte fibers and their controlled release properties. *Colloids And Surfaces B-Biointerfaces* 2007, *58* (2), 172-179; (c) Liu, H.; Kameoka, J.; Czaplewski,Ä¶, D. A., Polymeric nanowire chemical sensor. *Nano Letters* 2004, *4* (4), 671-675.

[2] Doshi, J.; Reneker, D., Electrospinning process and applications of electrospun fibers. *Journal of Electrostatics* 1995, *35* (2-3), 151-160.

[3] (a) Reneker, D.; Yarin, A.; Fong, H.; Koombhongse, S., Bending instability of electrically charged liquid jets of polymer solutions in electrospinning. *Journal of Applied Physics* 2000, *87*, 4531; (b) Rutledge,G, Formation of fibers by electrospinning. *Advanced Drug Delivery Reviews* 2007, *59* (14), 1384-1391.

[4] Fong, H.; Chun, I.; Reneker, D. H., Beaded nanofibers formed during electrospinning. *Polymer* 1999, (40), 4585-4592.

[5] Raghavan, B. K.; Coffin, D. W., Control of Inter-fiber Fusing for nanofiber Webs via Electrospinning. *Journal of Engineered Fiber and Fabrics* 2011, *6* (4), 1-5.

[6] (a) Kim, B.; Park, H.; Lee, S.; Sigmund, W., Poly (acrylic acid) nanofibers by electrospinning. *Materials letters* 2005, *59* (7), 829-832; (b) Li, L.; Hsieh, Y. L., Ultra-fine polyelectrolyte fibers from electrospinning of poly (acrylic acid). *Polymer* 2005, *46*, 5133-5139.

[7] Alivisatos, A., Semiconductor clusters, nanocrystals, and quantum dots. *Science* 1996, *271* (5251), 933.

[8] Yu, M.; Van Orden, A., Enhanced Fluorescence Intermittency of CdSe-ZnS Quantum Dot Clusters. *Physical Review Letters* 2006, *97*, 23702-4.

[9] Hara, M., *Polyelectrolytes: science and technology* Marcel Dekker, Inc.: New York, 1993.

[10] Lundberg, R. D.; Phillips, R. R., Solution behavior of metal sulfonate ionomers.II Effects of solvents. *J. Polym.Sci. Polym. Phys. Ed.* 1982, *20*, 1143.

[11] Han, T.; Reneker, D. H.; Yarin, A., Buckling of jets in electrospinning. *Polymer* 2007, *48*, 6064-76.

[12] Atchison, J. S.; Schauer, C. L., Fabrication and characterization of electrospun semiconductor nanoparticle-polyelectrolyte ultra fine fiber composites for sensing applications. *Sensors* 2011, *11* (10) 10372-10387.

[13] Demir, M. M.; Soyal, D.; Ünlü, C.; Kus, M.; Özçelik, S., Controlling Spontaneous Emission of CdSe Nanoparticles Dispersed in Electrospun Fibers of Polycarbonate Urethane. *J. Phys. Chem C* 2009, *113*, 11273.

AUTHORS' ADDRESSES

Jennifer S. Atchison
Caroline L. Schauer, Ph.D.
Department of MSE Drexel University
Drexel University
3141 Chestnut St
Philadelphia, PA 19104